

Distribution of stratospheric column ozone (SCO) determined from satellite observations: Validation of solar backscattered ultraviolet (SBUV) measurements in support of the tropospheric ozone residual (TOR) method

Amy E. Wozniak,¹ Jack Fishman, Pi-Huan Wang,² and John K. Creilson¹

NASA Langley Research Center, Hampton, Virginia, USA

Received 4 February 2005; revised 18 July 2005; accepted 27 July 2005; published XX Month 2005.

[1] The global (50°N–50°S) distribution of stratospheric column ozone (SCO) is derived using solar backscattered ultraviolet (SBUV) profiles and compared with SCO amounts derived from Stratospheric Aerosol and Gas Experiment (SAGE) and ground-based measurements. An evaluation of archived SBUV (version 6) ozone profiles with ozonesonde profiles shows that the low resolution of the SBUV instrument in the troposphere and lower stratosphere leads to a low bias in the SBUV profile in the troposphere and a high bias in the lower stratosphere in regions where anthropogenic tropospheric ozone production influences the climatology. An empirical correction applied to the SBUV profile prior to separating the stratosphere from the troposphere reduces the bias in the lower stratosphere and results in a SCO distribution in good agreement with SCO derived from SAGE ozone profiles. Because the empirical correction is most pronounced at northern middle latitudes, we compare these resultant SCO values with those measured at two northern middle latitude sites (Wallops Island and Hohenpeissenberg) using concurrent measurements from Dobson spectrophotometers and ozonesondes. Our analysis shows that the empirically corrected SCO at these sites captures the seasonal cycle of SCO as well as the seasonal cycle derived from SAGE stratospheric ozone profiles. These results have important implications for the derivation of tropospheric ozone from SBUV ozone profiles in conjunction with Total Ozone Mapping Spectrometer (TOMS) total ozone measurements using the tropospheric ozone residual (TOR) methodology.

Citation: Wozniak, A. E., J. Fishman, P.-H. Wang, and J. K. Creilson (2005), Distribution of stratospheric column ozone (SCO) determined from satellite observations: Validation of solar backscattered ultraviolet (SBUV) measurements in support of the tropospheric ozone residual (TOR) method, *J. Geophys. Res.*, 110, DXXXXX, doi:10.1029/2005JD005842.

1. Introduction

[2] Determination of the global distribution of tropospheric ozone is central to gaining a fundamental understanding of tropospheric chemistry and to assessing how human activity has perturbed the composition of the pre-industrial atmosphere [e.g., see *Crutzen*, 1974; *Fishman and Crutzen*, 1978]. Attempts to produce a global distribution were first described in a series of studies in the 1970's using data from surface stations [*Fabian and Pruchniewicz*, 1973, 1977] and subsequently from analyses of ozonesonde measurements [*Chatfield and Harrison*, 1977; *Fishman et al.*, 1979]. Because of the variability inherently present in its distribution and abundance of tropospheric ozone,

Prinn [1988] recognized the difficulty in obtaining a representative depiction by using only surface and ozonesonde measurements and suggested that a considerable international effort be initiated to derive an accurate global picture using conventional in situ measurement techniques. Although some progress has been made through the establishment of a number of ozonesonde stations at low latitudes through the SHADOZ (Southern Hemisphere Additional Ozonesondes) network [*Thompson et al.*, 2003], many regions on the planet are significantly still undersampled.

[3] In addition, an alternative approach to derive a global picture of tropospheric ozone using satellite information was introduced by *Fishman et al.* [1990] using concurrent observations of total ozone and a stratospheric ozone profile from independent satellite instruments to derive a quantity called the tropospheric ozone residual (TOR). Although the TOR did not yield any information about the vertical distribution of ozone within the troposphere, it did provide unique insight into the latitudinal, longitudinal and seasonal variability of the column abundance of tropospheric ozone.

¹Also at Science Applications International Corporation (SAIC), Hampton, Virginia, USA.

²Also at Science and Technology Corporation, Hampton, Virginia, USA.

[4] Global data sets of atmospheric trace gases using satellite observations have been primarily constrained to distributions in the stratosphere [Kaye and Fishman, 2003] since making measurements at these relatively higher altitudes is much simpler than in the troposphere. Validation of these stratospheric data products has been critical to the assessment of stratospheric ozone depletion and a monumental amount of research has been conducted to assess the accuracy of stratospheric ozone derived from satellites as well as determining how well various satellite techniques compare to one another [World Meteorological Organization (WMO), 1999, 2003]. Thus we describe how relatively abundant stratospheric ozone profiles from satellite instruments such as SAGE (Stratospheric Aerosol and Gas Experiment) and SBUV (Solar Backscattered Ultraviolet) have been used to derive global TOR distributions, and then, as an alternative to explicitly validating the global TOR distribution, we assess the other component that comes out of TOR derivation, namely the global distribution of stratospheric column ozone (SCO). In the following sections we describe the methodology for deriving SCO from SBUV measurements, and validate the SBUV SCO through a comparison with SCO derived from SAGE measurements and with a comparable SCO quantity derived from concurrent ozonesonde and ground-based total ozone measurements.

2. TOR Method

[5] The first TOR method described by Fishman et al. [1990] used concurrent observations of total ozone from TOMS (Total Ozone Mapping Spectrometer) and stratospheric ozone profiles from SAGE to generate climatological maps of tropospheric column ozone. These depictions provided insight into how the seasonal tropospheric ozone distribution was influenced on hemispheric spatial scales by biomass burning in southern Africa and South America in the Southern Hemisphere, and by anthropogenic pollution sources from North America and Europe [Fishman et al., 1990] in the Northern Hemisphere. Whereas using TOMS and stratospheric ozone profile data from SAGE and SAGE II archives could generate climatological TOR maps, generation of TOR fields with better temporal resolution requires a higher sampling frequency than the 30 daily occultations available from the SAGE instruments [Vukovich et al., 1996]. The 40-day period required by SAGE to acquire pole-to-pole coverage precludes the possibility for deriving synoptic pictures on shorter timescales.

[6] The eruption of Mount Pinatubo in June 1991 prohibited the SAGE instrument from making accurate measurements in the lower stratosphere because of abnormally heavy aerosol loading, and thus TOR fields generated using concurrent measurements from TOMS and SBUV were derived for comparison with field measurements from NASA's 1992 Transport and Atmospheric Chemistry near the Equator-Atlantic (TRACE-A) mission [Fishman et al., 1996b], a field campaign motivated by the first TOMS/SAGE TOR findings of elevated ozone over the tropical South Atlantic Ocean [Fishman et al., 1996a]. The advantage of using SBUV data to derive stratospheric information for generating daily TOR fields is the global coverage (700–800 profiles daily) provided by the instrument. On

the other hand, the vertical resolution of the SBUV measurement below the ozone peak is less than that of the SAGE instrument, and this method has been shown to have significant shortcomings when archived (version 6) SBUV data are used [Vukovich et al., 1997; Ziemke et al., 1998].

[7] Because of these noted shortcomings in the archived SBUV data, Fishman and Balok [1999] modified the archived SBUV profiles in the lower atmosphere by applying an “empirical correction” to the lowest three layers of the profiles. The Fishman and Balok study focused on the regional distribution of tropospheric ozone over the eastern United States and used ozonesonde information from Wallops Island (Virginia) to apply “corrections” to every archived SBUV profile used in the study. The empirical correction technique was then expanded from a regional to near-global domain (50°N to 50°S) of Fishman et al. [2003] where the analyses derived by Logan [1999] were used to modify the archived SBUV profiles. It should be noted that the Logan tropospheric ozone climatology uses the global ozonesonde database as the primary input to drive her analysis. The resultant TOR distribution derived from TOMS and empirically corrected version 6 SBUV profiles (EC-TOR) made it possible to identify tropospheric regional scale ozone enhancements over a number of highly polluted regions (e.g., eastern United States, northern India, central Brazil, western Africa and central China).

[8] Subsequent to our use of the empirical correction to generate the TOR fields discussed by Fishman et al. [2003] and the SCO fields that will be discussed in the following sections, NOAA released a new archived SBUV data set (version 8). The primary improvement in the version 8 algorithm is an updated ozone profile climatology. Whereas the old climatology was based on three latitude zones (low, middle, and high) and total ozone amount, the new ozone profile climatology divides profiles into 10° latitude zones (90°S to 90°N), altitude, and monthly averages. The new climatology also incorporates an updated balloonsonde climatology (1988–2002) in the troposphere and lower stratosphere, and SAGE II and MLS data in the middle and upper stratosphere [McPeters et al., 2003]. A comparison of version 8 and version 6 profiles used in this study is presented in Appendix A.

3. Validation of the TOR Method and Purpose of this Study

[9] Since Fishman et al. [1990], there have been a number of studies that have used variations of the original TOMS/SAGE approach [Ziemke et al., 1998; Hudson and Thompson, 1998; Newchurch et al., 2001, 2003]. Each technique uses TOMS measurements to derive total column ozone and an additional measurement to define the stratospheric component of the total column to determine tropospheric ozone. The recent commentary by deLaat and Aben [2003] and the subsequent discussion by Fishman et al. [2003] highlight the difficulty of validating TOR data against currently available databases. Validation of its near-global distribution without space-based measurements of similar resolution is extremely difficult and requires the continual deployment of near-earth instruments capable of measuring ozone columns throughout the entire troposphere (i.e., ozonesondes, aircraft profiles and UV-DIAL lidar

t1.1 **Table 1.** Definition of SBUV Ozone Profile Layers

t1.2	SBUV Layer	Pressure Range, hPa	Midpoint Pressure, hPa	Approximate Midpoint Altitude, km
t1.3	1	253–1013	507	5.5
t1.4	2	127–253	179	12.5
t1.5	3	63.3–127	89.6	17.0
t1.6	4	31.7–63.3	44.8	21.3
t1.7	5	15.8–31.7	22.4	25.8
t1.8	6	7.92–15.8	11.2	30.4
t1.9	7	3.96–7.92	5.60	35.2
t1.10	8	1.98–3.96	2.80	40.2
t1.11	9	0.99–1.98	1.40	45.4
t1.12	10	0.495–0.099	0.700	51.0
t1.13	11	0.247–0.495	0.350	56.5
t1.14	12	0.0–0.2467

187 measurements [see *Fishman et al.*, 1996a, 1996b]). *Sun*
 188 [2002] presented an excellent discussion on the accuracy of
 189 the TOR method when compared to ozonesonde measure-
 190 ments, and he has provided an analysis to show how each
 191 method varies with one another. He concludes that each of
 192 the six methods displays comparable differences with data
 193 from tropical ozonesonde stations (the region of interest in
 194 his study). Although each of the techniques was able to
 195 discern higher values over the Atlantic than over the Pacific,
 196 *Sun* noted that all the methods tend to underestimate the
 197 amount of ozone over the Atlantic. The study goes on to
 198 conclude that all TOMS-based methods seem to capture the
 199 variance better than the absolute amount. The accuracy of
 200 the empirical correction technique of *Fishman et al.* [2003],
 201 the focus of this study, was not included as part of the
 202 comparison by *Sun* [2002].

203 [10] Subsequently, *deLaat and Aben* [2003] questioned
 204 the accuracy of the EC-TOR fields presented by *Fishman et al.*
 205 [2003] and the finding of the regional nature of enhanced
 206 tropospheric ozone amounts at subtropical and northern
 207 middle-latitude locations. As pointed out by *Fishman et al.*
 208 [2003], validation of TOR fields is extremely difficult
 209 without intensive dedicated field missions. On the other
 210 hand, the other product generated by the EC-TOR, namely
 211 the SCO, can be compared against available measurements
 212 derived from both in situ and satellite techniques. In turn,
 213 these satellite measurements have undergone intensive scruti-
 214 nity since they have been used to assess how much ozone has
 215 been destroyed owing to the release of chlorofluorocarbons
 216 [WMO, 1999, 2003]. Since EC-TOR uniquely provides a
 217 long-term data set at middle latitudes in addition to low
 218 latitudes (the limitations of other TOR techniques) a more
 219 robust comparison can be performed because of the much
 220 larger set of measurements (i.e., including NH midlatitude
 221 ozonesonde/ground-based sites) against which the EC-TOR
 222 can be compared. *Fishman and Balok* [1999] show that the
 223 EC-TOR agreed much better with ozonesonde data than the
 224 TOR using archived SBUV data. In the following sections,
 225 we additionally will show how the empirical correction to
 226 the SBUV archive has improved the accuracy of the SCO
 227 derived from the EC-TOR methodology.

228 4. Methodology for Deriving Stratospheric 229 Column Ozone From SBUV Profiles

230 [11] A challenge of using SBUV ozone profiles to derive
 231 stratospheric column ozone is in determining how to separate

the troposphere from the stratosphere given the low resolu- 232
 tion of the UV backscatter technique below the ozone peak. 233
 The following sections evaluate the dependence of the final 234
 profile on the a priori first-guess profile, compare the SBUV 235
 final solution profiles and ozonesonde measurements, and 236
 describe the empirical correction and its impact on the ozone 237
 profiles in the troposphere and lower stratosphere. 238

4.1. Ozone Profile Data 239

4.1.1. SBUV Ozone Profiles 240

[12] The SBUV instrument measures backscattered ultra- 241
 violet radiation at 12 different wavelengths to determine 242
 total ozone and the vertical ozone profiles. The SBUV 243
 instrument was launched on the NASA Nimbus-7 satellite 244
 and made measurements from November 1978 through 245
 June 1990. A similar record exists from January 1989 246
 through the present from a slightly modified SBUV/2 247
 instrument orbiting on the NOAA-11 satellite. The polar 248
 orbiting satellite platform provides global coverage every 6 249
 days. The SBUV data used in the study were derived using 250
 the version 6 inversion algorithm and archived as profile 251
 layer amounts (see Table 1). Details of the version 6 252
 retrieval algorithm and an error analysis of the SBUV ozone 253
 profiles are given by *Bhartia et al.* [1996]. 254

4.1.2. Ozonesonde Profile Measurements 255

[13] The ozonesonde data used in this study were 256
 obtained from the ozonesonde database maintained by 257
 NASA Langley Research Center (V. Brackett, NASA Lang- 258
 ley Research Center, personal communication, 2004). Stations 259
 chosen for comparison are between 50°N and 50°S 260
 (see Table 2) and have recurrent ozonesonde measurements 261
 from 1979 through 2000: Hohenpeissenberg, Sapporo, 262
 Sofia, Boulder, Wallops Island, Tateno, Kagoshima and 263
 Naha at northern midlatitudes; Nairobi and Natal at low 264
 latitudes; and Irene and Lauder at southern midlatitudes. A 265
 detailed description of the station data and the associated 266
 measurement error are presented by *Logan* [1999]. 267

4.2. Comparison of Archived SBUV Ozone Profiles With the A Priori First-Guess Profiles in the Troposphere 268 269 270

[14] The UV wavelengths used to determine the ozone 271
 profile in the troposphere and lower stratosphere are sensi- 272
 tive to aerosols, clouds and ozone over a broad range of 273
 altitudes. Such sensitivities limit the vertical resolution of 274
 the instrument to approximately 15 km below the peak, 275
 whereas the resolution above the peak is approximately 276

Table 2. Individual Stations With Ozonesonde and Ground-Based 22.1
 Total Ozone Measurements

WMO ID	Station Name	Latitude, deg	Longitude, deg	t2.2
099	Hohenpeissenberg, Germany	47.80 N	11.02 E	t2.3
012	Sapporo, Japan	43.05 N	141.33 E	t2.4
132	Sofia, Bulgaria	42.81 N	23.38 E	t2.5
067	Boulder, Colorado	40.03 N	105.25 W	t2.6
014	Tateno, Japan	36.05 N	140.13 E	t2.7
107	Wallops Island, Virginia	37.93 N	75.48 W	t2.8
007	Kagoshima, Japan	31.55 N	130.55 E	t2.9
190	Naha, Japan	26.20 N	127.68 E	t2.10
175	Nairobi, Kenya	1.27 S	36.80 E	t2.11
219	Natal, Brazil	5.42 S	35.38 W	t2.12
265	Irene, Pretoria, South Africa	25.90 S	28.22 E	t2.13
256	Lauder, New Zealand	45.03 S	169.68 E	t2.14

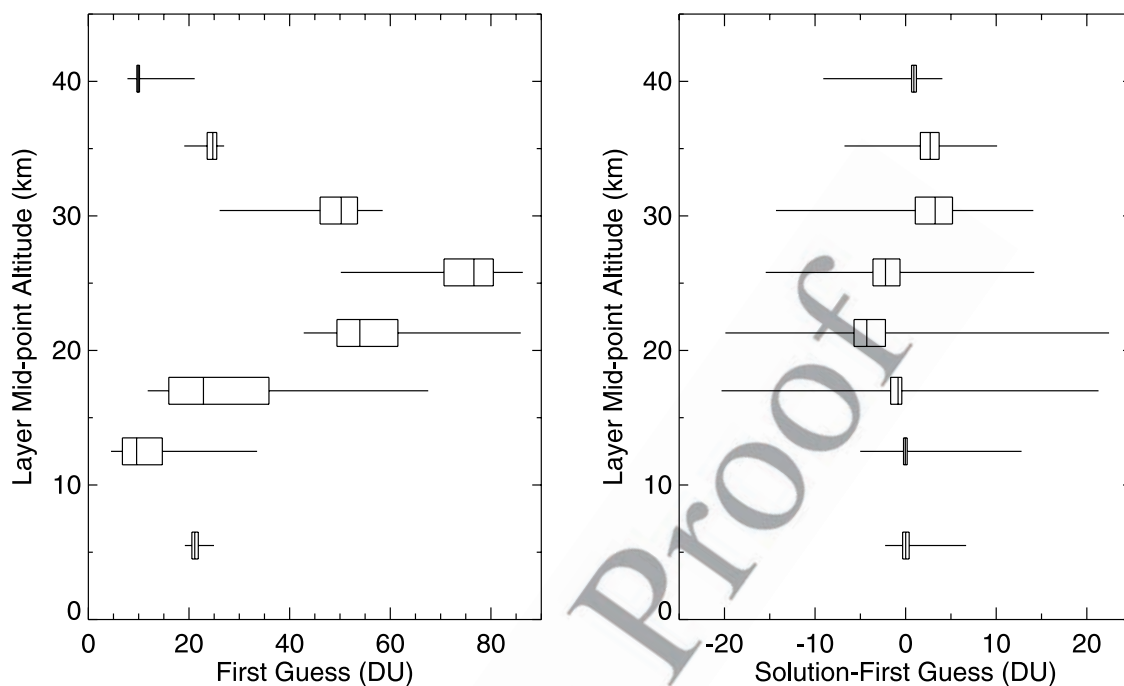


Figure 1. (left) A box-and-whiskers plot of the NOAA-11 1999 50°S to 50°N first-guess profile layers as a function of layer midpoint altitude. The left and right edges of the box show the lower and upper quartiles, respectively. The line through the middle of the box shows the median value and the whiskers show the minimum and maximum values for each layer. (right) A box-and-whiskers plot for the difference between the final solution profile and first-guess profile (final solution-first guess) for each layer.

277 8 km. The decreased sensitivity to ozone in the lower
 278 portion of the profile forces the retrieval algorithm to
 279 depend heavily on the a priori first-guess profile shape
 280 and the total ozone amount in determining the final profile
 281 below the ozone peak [McPeters *et al.*, 1986]. The version 6
 282 SBUV retrieval a priori first-guess profiles are classified by
 283 total ozone and latitude and derived from SAGE and
 284 ozonesonde profiles. Figure 1 shows a box-and-whisker
 285 plot of the NOAA-11 1999 50°S to 50°N first-guess ozone
 286 profile layers (Figure 1, left) and the difference between the
 287 final solution profile and first-guess profile for each layer
 288 (Figure 1, right). The graphs show data from over 200,000
 289 profiles. The left and right edges of the box are the upper
 290 and lower quartiles of the difference and the line through the
 291 middle of the box is the mean. The whiskers extend to the
 292 minimum and maximum values. Figure 1 shows that the
 293 first-guess Layer 1 has the least variable climatology below
 294 the ozone peak and that the majority of the variability in the
 295 profile shape, and therefore total column ozone, comes from
 296 Layers 2 through 6. It is clear from Figure 1 (left) that the
 297 first-guess value of Layer 1 ranges from approximately 20
 298 DU to 25 DU and from Figure 1 (right) that the range of the
 299 final solution profile is within -2 DU to $+6$ DU of the first-
 300 guess value with a most probable value of zero. We will
 301 show in the following comparison of SBUV profiles with
 302 ozonesonde profiles that owing to the limited a priori first-
 303 guess climatology, the Layer 1 final solution is generally
 304 lower than the climatological ozonesonde value and also
 305 lacks the seasonal variability seen in the in situ measure-
 306 ments [e.g., see *Fishman and Balok*, 1999, Plates 1 and 2].

Conversely, the final solution to Layer 3 is nearly always
 higher than that of the ozonesonde values.

4.3. Comparison of SBUV Ozone Profiles With Ozonesonde Measurements in the Troposphere and Lower Stratosphere

[15] The following results are quantitative comparisons of
 the combined 16-year Nimbus-7 and NOAA-11 archived
 version 6 SBUV ozone profile data set with an ozonesonde
 profile data set consisting of more than 3000 measurements
 from 12 stations at middle to low latitudes. The high-
 resolution ozone soundings were integrated to obtain the
 layers defined in Table 1. SBUV profile measurements were
 required to be within 5° latitude by 5° longitude of the
 ozonesonde station location and on the same day as the
 ozonesonde launch. The comparison focuses on Layers 1
 through 5 since most ozonesondes burst before reaching
 15.8 hPa. Layer 1 represents the amount of ozone in the
 troposphere. Layers 2 and 3, depending on latitude and
 tropopause height, can be a mix of tropospheric and
 stratospheric air. Layers 4 and 5 are representative of
 stratospheric concentrations at the ozone profile maximum.

[16] Figure 2 shows the mean difference (SBUV-Ozone-
 sonde) and standard deviation of the SBUV layer amounts
 compared with ozonesonde measurements. Positive differ-
 ences indicate SBUV is overestimating the amount of ozone
 in the layer, and negative differences indicate SBUV is
 underestimating the amount of ozone in the layer. In the
 previous section we determined that there is little if any
 change in Layer 1 ozone from the first-guess climatology to

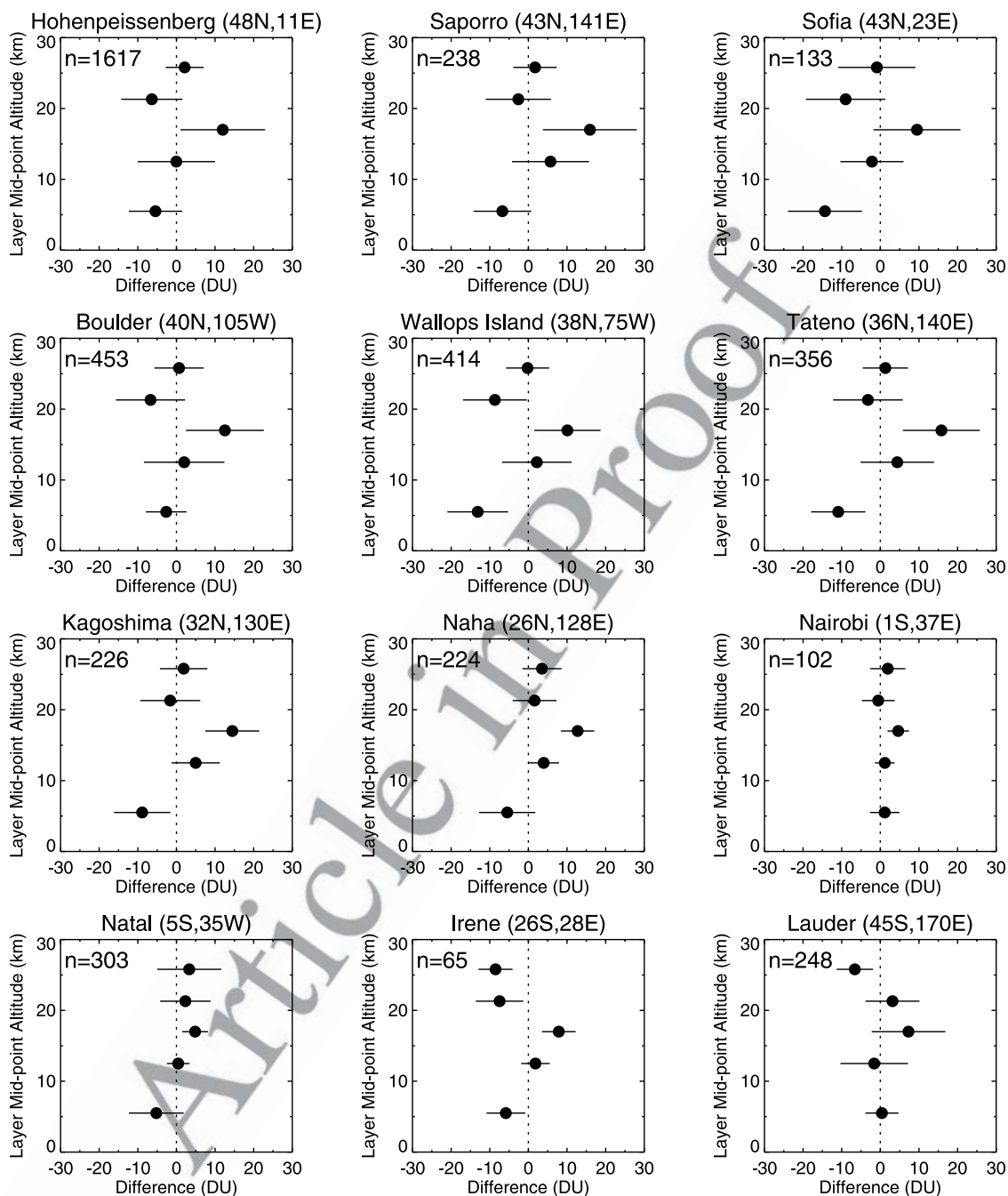


Figure 2. Mean difference (SBUV-Ozonesonde) for archived version 6 SBUV Layers 1 through 5 when compared with ozonesonde profiles. The solid bars represent 1-sigma standard deviation from the mean.

336 the final solution profile, therefore differences in SBUV and
 337 ozonesonde values can be directly attributed to the first-
 338 guess climatology. At 10 of the 12 ozonesonde stations used
 339 in the comparison, the amount of ozone in SBUV Layer 1 is
 340 less than the amount of ozone in the ozonesonde Layer 1
 341 and conversely, the amount in ozone in SBUV Layer 3 is
 342 greater than the amount of ozone in the ozonesonde Layer 3.
 343 Given that the integral of the lowest 3 Layers is a truer
 344 representation of the vertical resolution of the instrument,
 345 Figure 2 suggests that excess ozone below the ozone peak is
 346 erroneously placed in Layer 3 owing to the invariant Layer
 347 1 first-guess climatology.

[17] Tropospheric ozone production increases in the 348
 Northern Hemisphere during the summer months (JJA) 349
 owing to photochemical production associated with anthro- 350
 pogenic emissions of NO_x and CO [Wang *et al.*, 1998]. The 351
 seasonal nature of excess tropospheric ozone production 352
 should produce a seasonal trend in the mean difference 353
 between the Layer 1 and Layer 3 SBUV ozone and 354
 comparable ozonesonde amounts. Figure 3 shows the 355
 monthly mean differences of SBUV Layer 1 and Layer 3 356
 ozone amounts compared with ozonesonde values (SBUV- 357
 Ozonesonde). At the midlatitude Northern Hemisphere 358
 stations of Hohenpeissenberg (48°N), Saporro (43°N), Sofia 359

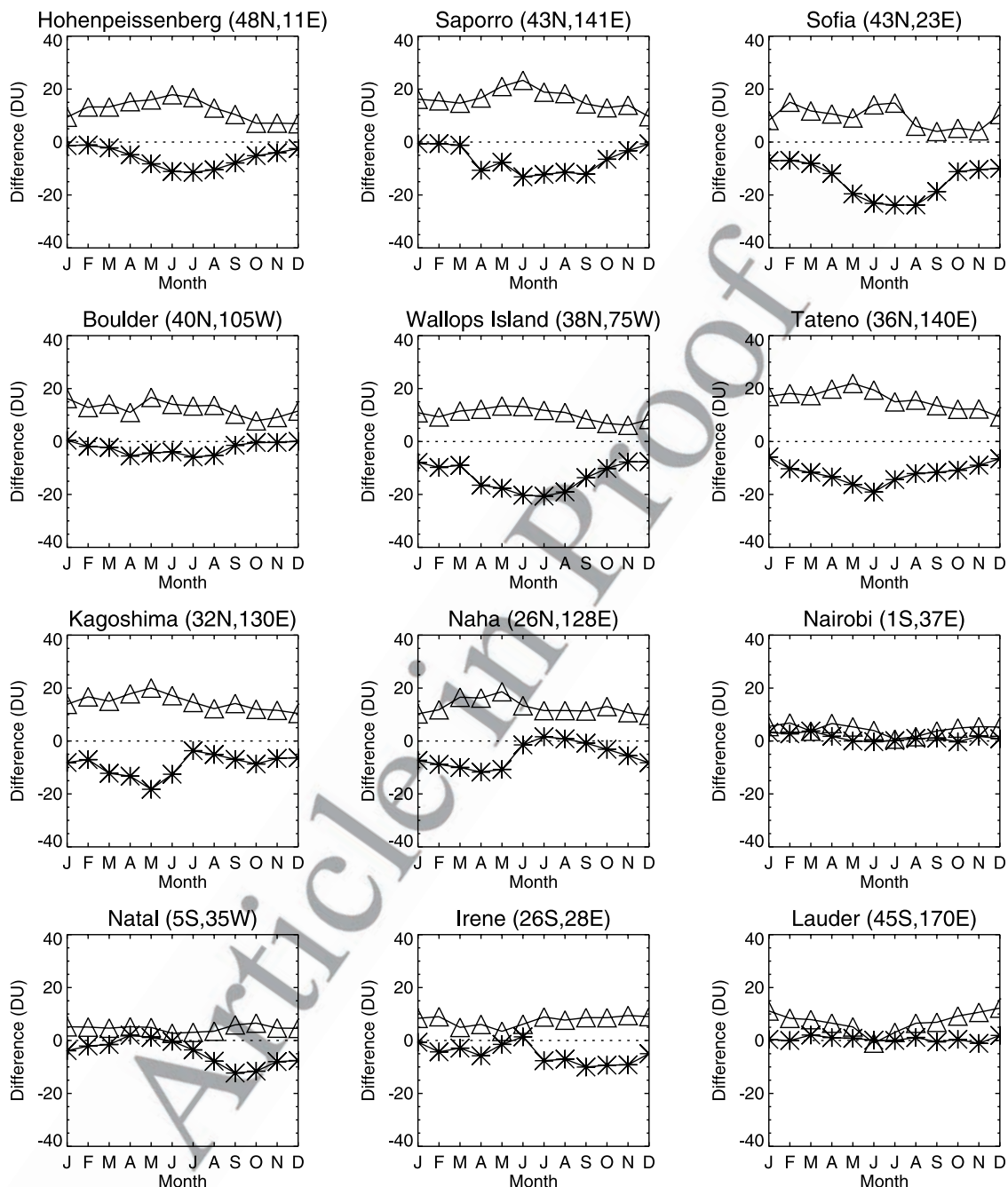


Figure 3. Monthly mean differences between of SBUV profiles and ozonesonde profiles (SBUV-ozonesonde) in Layer 1 (asterisks) and Layer 3 (triangles).

360 (43°N), Boulder (40°N), Wallops Island (38°N), and Tateno
 361 (36°N), the difference between the satellite and ozonesonde
 362 measurements of Layer 1 are greatest during the June, July
 363 and August (JJA) summertime ozone maximum. This
 364 seasonal mean difference between SBUV and ozonesondes
 365 in Layer 1 is less pronounced at Boulder than the other
 366 midlatitude Northern Hemisphere stations owing to its high-
 367 altitude location. The Boulder station is located 1634 m
 368 above sea level which will bias the ozonesonde integral
 369 between 1013 hPa and 253 hPa (Layer 1) low compared to
 370 the other stations at similar latitude.

371 [18] In contrast to the higher latitude Japanese stations of
 372 Saporro and Tateno, lower latitude stations Kagoshima

(32°N) and Naha (26°N) show the mean difference in Layer
 373 1 is a maximum during the spring in May and minimum
 374 during the summer in July. Layer 3 shows similar seasonal
 375 behavior. These stations have a maximum in ozone in
 376 spring, which coincides with increased photochemical pro-
 377 duction of ozone. The sharp decline in the difference in June
 378 and July is due to the summer monsoon pattern of low
 379 ozone air from the tropical Pacific being advected onto the
 380 island [Logan, 1985, 1999].
 381

[19] At the two South Atlantic stations of Natal (5°S) and
 382 Irene (26°S), maximum mean differences are shifted into
 383 austral spring (September–November), coincident with the
 384 peak of biomass burning. South American and African
 385

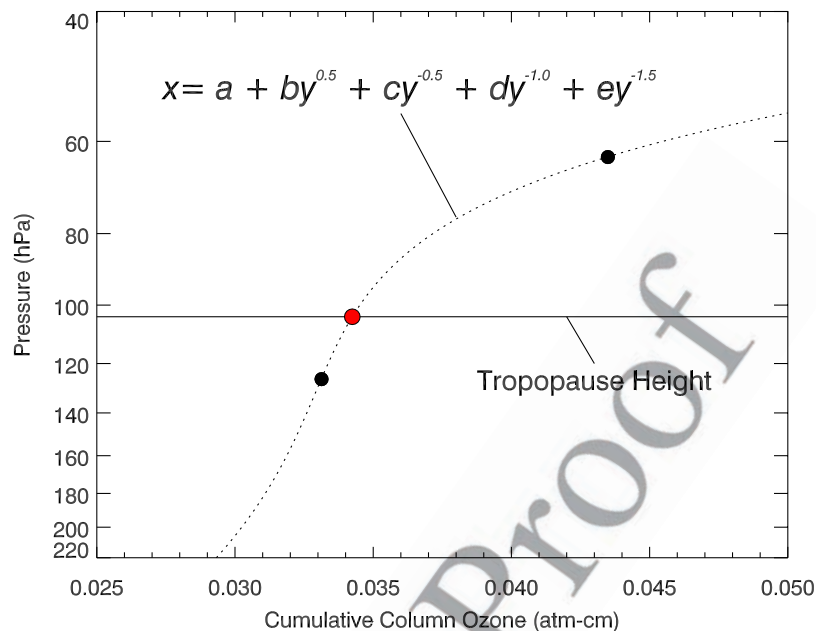


Figure 4. Interpolation of the cumulative SBUV ozone to the tropopause pressure using a fifth-order polynomial. The solid black circles represent the cumulative SBUV ozone at the top of Layers 2 and 3. The solid red circle represents the interpolated cumulative amount of ozone at the tropopause pressure using the fifth-order polynomial.

386 biomass burning, respectively, influence Natal and Irene.
 387 Irene is another station, like Boulder, with a low bias in
 388 Layer 1 compared with other stations at the same latitude
 389 because the site is 1523 m above sea level. Irene is
 390 influenced by African biomass burning in austral spring
 391 and year-round by anthropogenic emissions from Pretoria
 392 and Johannesburg [Diab *et al.*, 2004]. A strong seasonal
 393 correlation between ozone and CO measurements from
 394 MOPPIT exists at both locations [Bremer *et al.*, 2004].

395 [20] At the two Pacific stations of Nairobi (1°S) and
 396 Lauder (45°S), differences are close to zero in Layer 1
 397 and show only slight differences in Layer 3. The Nairobi
 398 ozonesonde station is part of the SHADOZ network, and the
 399 tropospheric columns are lower than other SHADOZ sta-
 400 tions that may be influenced by African biomass burning
 401 sources. Thompson *et al.* [2003] cite two possible reasons
 402 for this difference: First, high terrain removes approximately
 403 3–5 DU of ozone since the elevation of the Nairobi station is
 404 1795 m; second, Thompson *et al.* show, through 5-day back
 405 trajectories at 500 hPa, that Nairobi is influenced primarily
 406 by air masses with origins east of the continent over the
 407 Indian Ocean and not from air re-circulated over southern
 408 Africa. The ozonesonde station at Lauder exhibits minimal
 409 seasonal variability in tropospheric ozone and is in excellent
 410 agreement with the SBUV first-guess climatology in Layer
 411 1. Layer 3 differences increase during Southern Hemisphere
 412 summer (DJF), consistent with previous findings when this
 413 layer was compared with profiles derived from SAGE at
 414 these latitudes [McPeters *et al.*, 1994].

415 4.4. Application of Empirical Correction to the 416 SBUV Profiles

417 [21] We have shown that the amount of ozone in the
 418 lower stratosphere in SBUV Layer 3 from 127 hPa to

63 hPa is consistently overestimated when compared to the
 419 ozonesonde climatology and conversely, the lowest layer in
 420 the SBUV profile, Layer 1, from 1013 hPa to 253 hPa is
 421 consistently underestimated when compared with the ozone
 422 climatology at stations where excess photochemical produc-
 423 tion of ozone contributes significantly to the climatology.
 424 This finding prompted the use of an empirical correction to
 425 the SBUV profiles to reduce the seasonal bias in Layer 3
 426 based on a monthly climatology developed by Logan [1999]
 427 and described by Fishman *et al.* [2003]. Since the final
 428 solution profile contains no information in the troposphere,
 429 we replace the SBUV Layer 1 and Layer 2 with the Logan
 430 climatology and apply the residual as a correction to the
 431 lower stratosphere (Layer 3). The tropospheric portion of the
 432 profile is prescribed as a function of geographic location and
 433 month of the year. It takes into account regional and seasonal
 434 tropospheric enhancements that were not included in the
 435 version 6 a priori first-guess ozone profiles, which were
 436 based solely on total ozone and latitude. The empirically
 437 corrected ozone profile is then integrated to the NCEP
 438 tropopause pressure. The tropopause pressure will vary
 439 according to global location and time of year and will
 440 generally lie within Layer 2 or Layer 3.
 441

442 [22] An illustration of how the interpolation within Layer
 443 3 is applied is shown in Figure 4. We have developed a
 444 fifth-order polynomial fit between Layer 2 and Layer 3 that
 445 predicts the cumulative amount of ozone as a function of
 446 pressure. Using the curve defined by the polynomial, the
 447 amount of integrated ozone below the tropopause is calcu-
 448 lated using the NCEP tropopause height information. That
 449 quantity is then subtracted from the SBUV total ozone
 450 amount to define the SCO. The estimated error associated
 451 with the interpolation based on testing with over 11000
 452 ozonesondes (not limited to the 12 stations used in this

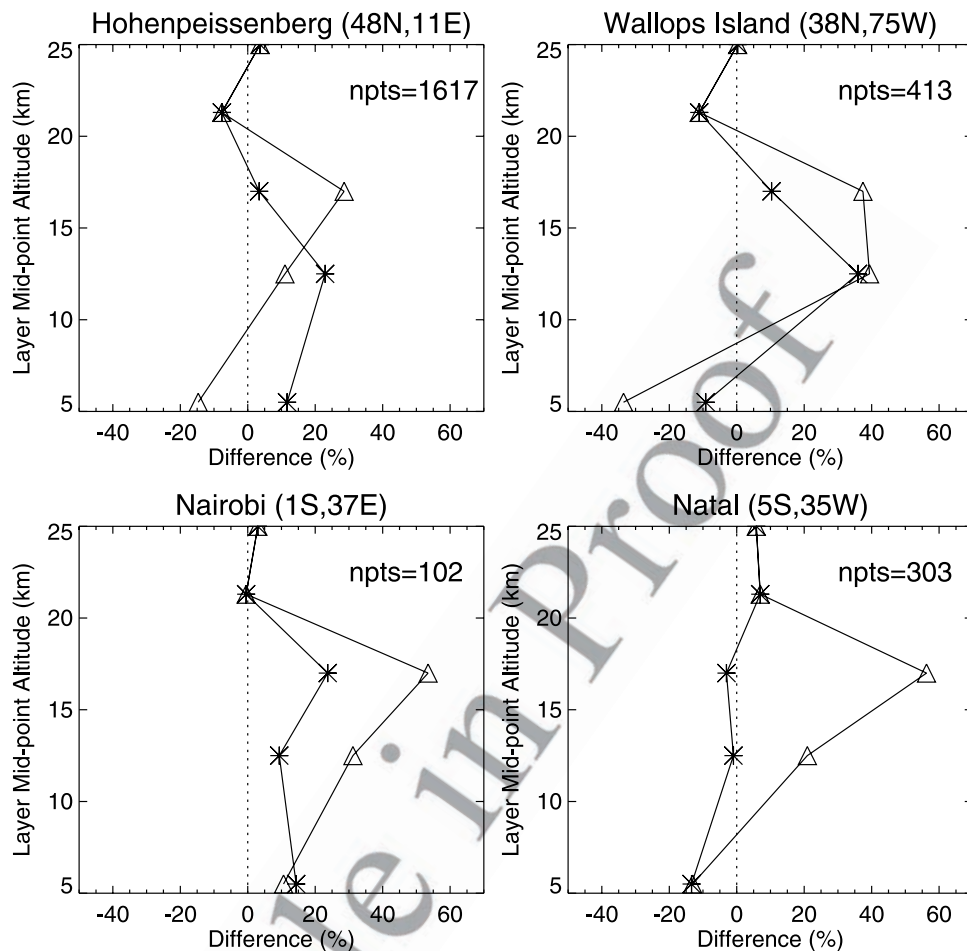


Figure 5. Mean bias of SBUV profiles compared with ozonesonde profiles (SBUV-ozonesonde/ozonesonde) for Layers 1–5 at four locations. Triangles are uncorrected SBUV profiles and asterisks and corrected SBUV profiles.

453 study) launched between 1996 and 2003 is 0 ± 2 DU.
 454 Figure 5 summarizes the mean difference between the
 455 archived and empirically corrected SBUV layers and
 456 corresponding ozonesonde layers for four stations ranging
 457 in latitude from 47°N to 5°S . The empirical correction has
 458 lowered the bias in Layer 3 at all stations.

459 [23] The residual methodology relies on each individual
 460 SBUV ozone profile measurement to compute the SCO
 461 and capture the large-scale synoptic patterns that define
 462 the stratospheric ozone distribution. By applying the
 463 empirical correction to the lowest three layers of the
 464 ozone profile we can improve calculation of the strato-
 465 spheric column ozone by improving the retrieved ozone
 466 profile in the troposphere and lower stratosphere (Layers 1
 467 through 3). It is possible that other perturbations in the
 468 profile radiances can cause the overestimation of the lower
 469 stratospheric layer, which would not be remedied through
 470 the application of the empirical correction. On the other
 471 hand, we can show that the resultant SCO distribution is
 472 an improvement over the SCO derived from archived
 473 SBUV profiles. The uniqueness of the SBUV record and
 474 the plans for continued SBUV instrument measurements
 475 encourages us to continue investigating the value of
 476 SBUV ozone profile measurements for determining strato-

spheric column ozone and its usefulness in the derivation 477
 of tropospheric ozone fields in conjunction with total 478
 column ozone from TOMS. 479

5. Validation of SBUV Derived Stratospheric Column Ozone 481

482
 [24] Although satellite measurements provide much better 483
 temporal and spatial resolution than individual ground 484
 measurement stations, validation of the resultant satellite 485
 distributions is intrinsically challenging. Accurate measure- 486
 ments of the entire stratospheric column are difficult to 487
 achieve from any one instrument. Ground-based methods 488
 (e.g., lidar) can experience interference from atmospheric 489
 aerosols and pollution, or be limited in altitude range; 490
 similarly, satellite-based measurements typically lose accu- 491
 racy at lower altitudes owing to radiative interference from 492
 multiple sources. Thus we have chosen two methods to test 493
 the validity of SBUV SCO data set: comparison against 494
 other independently derived quantities (as in the previous 495
 section) and a comparison with fields derived from another 496
 satellite data set which we know correctly captures the 497
 vertical structure throughout the stratosphere. For this latter 498
 portion of the validation study, we compare the EC-SBUV 499

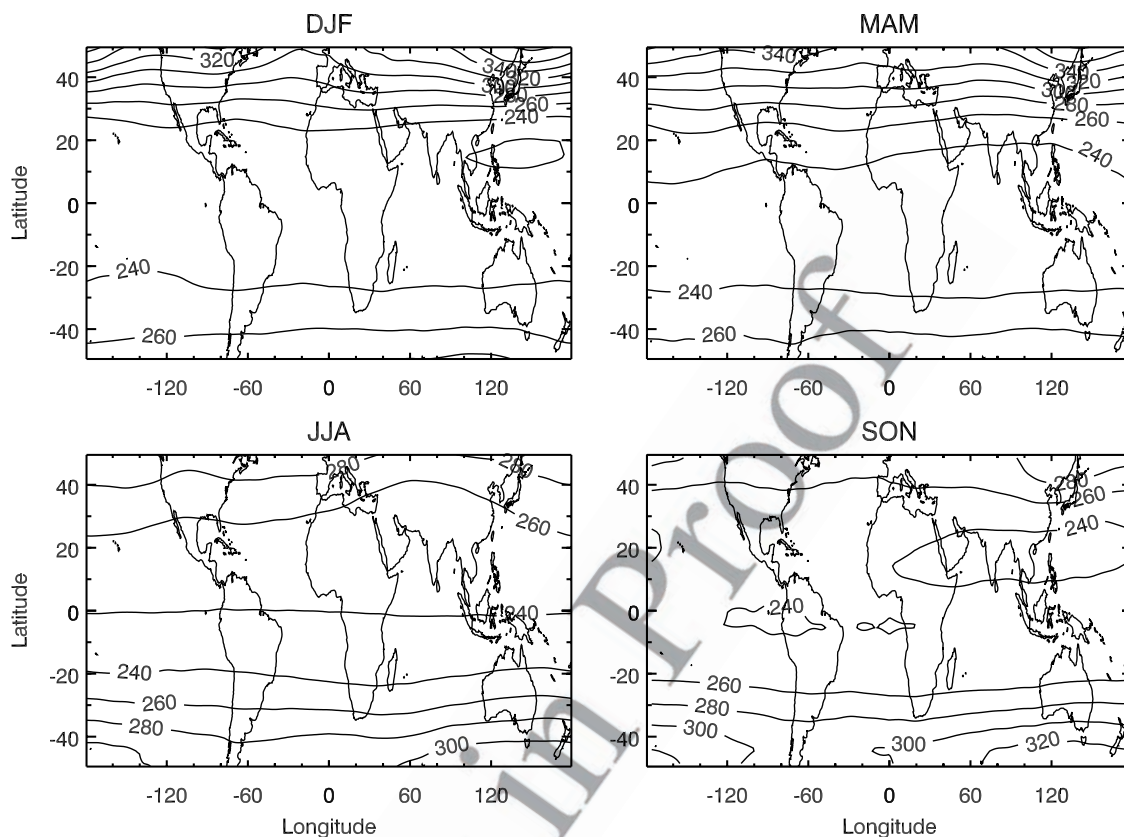


Figure 6. Seasonal stratospheric column ozone distribution derived from SAGE II (1985–2000) ozone profiles.

500 SCO with SCO fields derived from SAGE profiles. The
501 results of this comparison are presented below.

502 5.1. Comparison of SBUV and SAGE Derived 503 Stratospheric Column Ozone Fields

504 [25] Stratospheric ozone profile measurements made from
505 SAGE II from 1985 through the present provide solar
506 occultation measurements of ozone profiles with much
507 higher vertical resolution than SBUV to derive stratospheric
508 column ozone. The SAGE ozone profile measurements
509 have been shown to be in agreement with ozonesonde
510 measurements to within 10% down to the tropopause [Wang
511 *et al.*, 2002].

512 [26] Figure 6 shows the seasonal stratospheric ozone
513 climatology derived from integrating high vertical resolu-
514 tion SAGE II profiles above the NCEP tropopause height.
515 Profile measurements from 1985 through 2000 were included
516 except for those in the 3 years following the June 1991
517 eruption of Mount Pinatubo. The dynamical movement of
518 the tropopause height is the primary determinant of the
519 stratospheric ozone column. The strongest gradients are
520 located in the vicinity of strong jet streams where strong
521 gradients in tropopause heights can be found. Most of the
522 ozone is located in the stratosphere, and the same gradients
523 in Figure 6 SCO from SAGE II can also be observed in the
524 total column ozone, particularly in the absence of chemical
525 production in the troposphere. SCO is lower in the tropics
526 owing to higher tropopause heights and therefore less mass
527 in the stratosphere. Outside of the tropics, the tropopause
528 height generally decreases toward the poles. Because the

tropopause height is determined from the temperature 529
profile, there are seasonal differences in the stratospheric 530
ozone fields between hemispheres. In the summer hemi- 531
sphere, stratospheric column ozone values are lower than in 532
the winter hemisphere. Stratospheric column ozone values 533
are larger in the Northern Hemisphere in winter (December 534
through February) and spring (March through May), than 535
during the summer (June through August) or fall (Septem- 536
ber through November) months. The same pattern is seen 537
during the Southern Hemisphere winter and spring (JJA and 538
SON) relative to austral summer and autumn (DJF and 539
MAM). The variability of the position of the midlatitude jet 540
stream and separation between tropical and midlatitude air 541
masses results in the stratospheric ozone gradient becoming 542
less zonal outside the tropics. The SCO minimum does not 543
occur exactly at the equator, but rather at the low latitudes of 544
the winter hemisphere. 545

[27] Figure 7 shows the seasonal stratospheric ozone 546
columns derived from Nimbus-7 SBUV and NOAA-11 547
SBUV/2 empirically corrected ozone profiles from 1985 548
through 2000 integrated above the NCEP tropopause height. 549
The SBUV seasonal climatologies show similar patterns of 550
increasing ozone toward the poles, the seasonal shift of the 551
minimum in the tropics, and the zonal asymmetry in the 552
midlatitudes. 553

[28] Figure 8 shows the differences in Dobson Units 554
between the SAGE and the EC-SBUV seasonal SCO 555
climatologies superimposed on the 500-hPa horizontal (u) 556
wind field. The solid contours indicate when EC-SBUV 557
SCO is high compared to SAGE and dashed contours 558

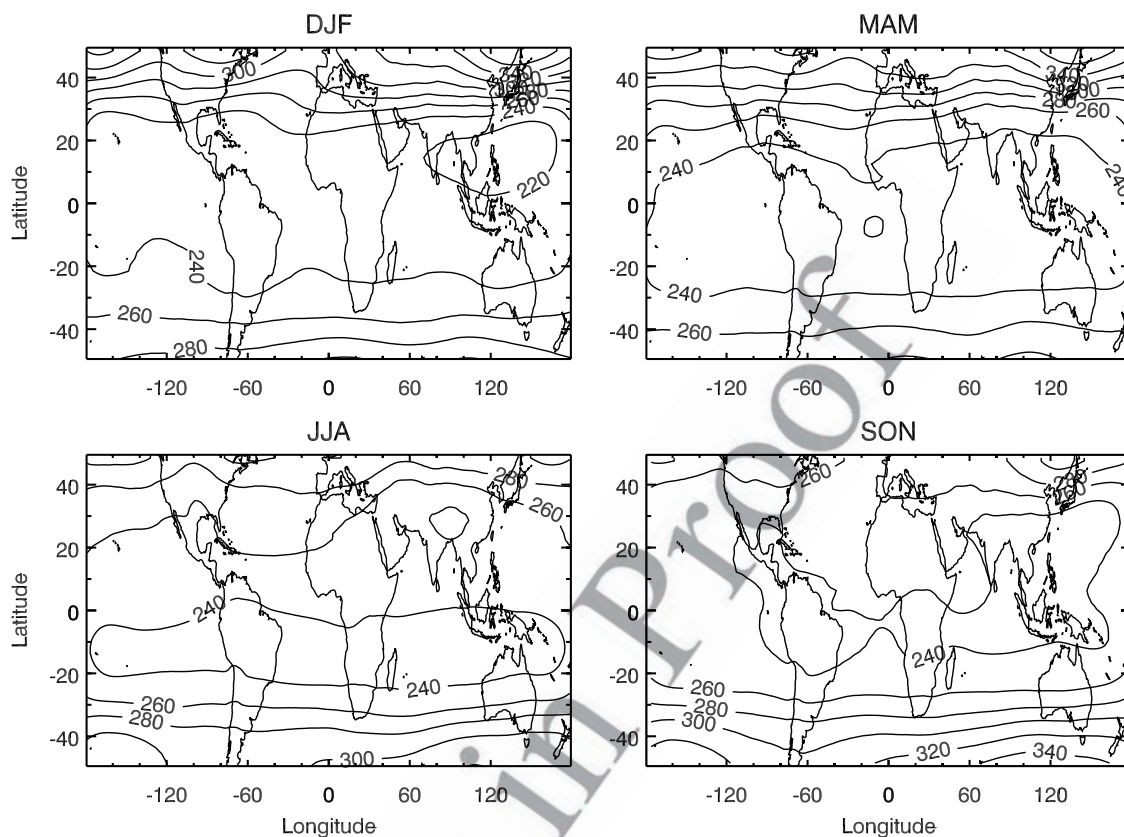


Figure 7. Same as Figure 6 except using data from empirically corrected SBUV measurements from 1985 through 2000.

559 indicate when EC-SBUV SCO is low compared to SAGE. 560 The greatest absolute differences occur at latitudes greater 561 than 40° in the Southern Hemisphere during SON and DJF. 562 These differences are consistent with comparisons of SAGE 563 and SBUV that show SBUV greater than SAGE in the 564 lower stratosphere by approximately 10% [McPeters et al., 565 1994; SPARC, 1998]. Other significant differences are in the 566 regions over the western Pacific Ocean east of the Asian 567 continent, and over the northwestern Atlantic off of the east 568 coast of the United States, and also south of Europe over 569 Northern Africa and western Asia. These features are 570 strongest in DJF and MAM, but generally persist through- 571 out the year. These three large differences coincide with 572 local maxima in the midlatitude jet stream.

573 [29] Figure 9 highlights improvement of the EC-SBUV 574 SCO over the archived SBUV SCO relative to the SAGE 575 SCO distribution (i.e., the quantity $|SBUV - SAGE| - 576 |EC-SBUV - SAGE|$). Regions with positive values indi- 577 cate where the EC-SBUV climatological value is now closer 578 to the SAGE climatological value. Improvements of more 579 than 5 DU are found over much of the Northern Hemisphere 580 and over the South Atlantic off the coast of Southern 581 Africa. The greatest improvement is over the Northern 582 Hemisphere during the summer months (JJA). Regions of 583 no improvement (negative values) are typically in the 584 midlatitude storm tracks. Above the surface (1000 hPa) at 585 northern midlatitudes ($>20^\circ N$), the Logan climatology is 586 zonally symmetric, and therefore will not reflect higher 587 ozone amounts in the upper troposphere in regions where

higher ozone amounts are present owing to enhanced 588 outflow from the stratosphere [Beekman et al., 1997]. 589

5.2. Comparisons of SBUV Derived Stratospheric 590 Column Ozone With In Situ and Ground-Based 591 Measurements 592

[30] In this section we compare empirically corrected 593 SBUV SCO with stratospheric columns derived from 594 coincident ground-based total ozone measurements and 595 integrated tropospheric column ozone from ozonesondes 596 using the WMO definition of the thermal tropopause height 597 for each sounding. The total ozone measurements used in 598 this study (also see Table 2) were obtained from the World 599 Ozone Data Center maintained by Environment Canada. 600 The daily total column ozone values for all stations except 601 Sofia, Bulgaria, were made with Dobson spectrometers. 602 The daily total column ozone from Sofia, Bulgaria, was 603 measured using a filter ozonometer. A discussion of the 604 different methods and comparisons of the ground-based 605 total ozone measurements with Nimbus-7 TOMS and 606 SBUV measurements is provided by Fioletov et al. [1999]. 607

[31] Figure 9 shows that the largest changes in SCO 608 resulting from the empirical correction take place at North- 609 ern Hemisphere (NH) middle latitudes, especially in spring 610 and summer. We compare satellite-derived SCO values with 611 SCO integrals generated at the NH middle latitude ozone- 612 sonde sites of Hohenpeissenberg ($47^\circ N$, $11^\circ E$) and Wallops 613 Island ($38^\circ N$, $75^\circ W$). For the data summarized in Tables 3a 614 and 3b and Figures 10a and 10b, 1347 ground-based obser- 615

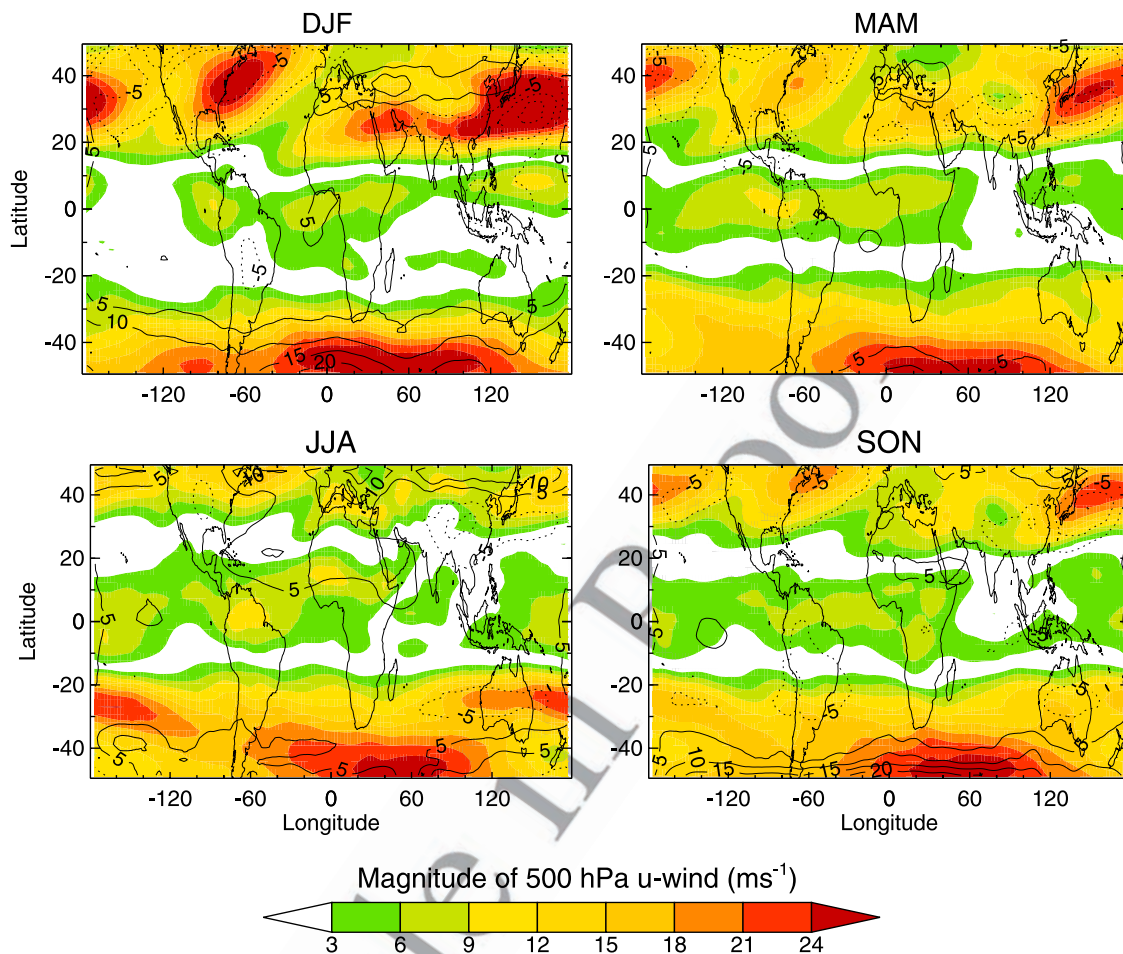


Figure 8. Solid and dashed contours depict the difference between EC-SBUV and SAGE (EC-SBUV – SAGE) stratospheric column ozone fields. The magnitude of the 500-hPa u-wind (m s^{-1}) is shown by the color contours.

616 vations were included in monthly averages at Hohenpeissen- 641
 617 berg and 416 at Wallops Island. SAGE profiles that were 642
 618 within 1000 km of each of the two stations were used in 643
 619 the analysis, resulting in 1031 profiles at Hohenpeissenberg and 644
 620 1488 profiles at Wallops Island. No coincident time crite- 645
 621 rion was imposed on the SAGE overpass and ozonesonde 646
 622 launch times, as this would have greatly diminished the 647
 623 number of profiles that could have been used to determine 648
 624 the monthly climatological values. Monthly SBUV values 649
 625 were calculated by averaging 17 years of daily SCO fields, 650
 626 interpolated to a 1.0° by 1.25° matrix, at the grid point 651
 627 closest to each of the ground station locations. 652

628 [32] Wang *et al.* [2002] performed a detailed comparison 647
 629 of coincident SAGE and ozonesonde profiles at Hohenpeis- 648
 630 senberg. Examination of 329 coincident profiles (which in 649
 631 their study meant within 24 hours and within ~ 1000 km) 650
 632 shows that there is excellent agreement between 13 and 651
 633 28 km, with the middle latitude stations generally within 652
 634 5% down to 20 km and within 10% down to 10 km. SAGE 653
 635 exhibits a positive bias between 15 and 20 km, which is 654
 636 consistent with our analysis, but the data presented in Table 655
 637 3a and Figure 10a suggest that this bias is most pronounced 656
 638 in November and December, the only 2 months where the 657
 639 SAGE-derived and the observed SCO from the Dobson- 658
 640 ozonesonde measurements differ by more than 20 DU. 659
 660
 661
 662
 663
 664
 665

641 During the rest of the year, the SAGE average is less than 642
 643 2 DU lower than the measured SCO. Wang *et al.* did not 644
 645 discuss the seasonality of the differences because effects of 646
 647 synoptic scale differences tended to mask the effects of 648
 649 seasonality differences (D. M. Cunnold, personal commu- 650
 651 nication, 2005). 652

647 [33] Without the empirical correction, Table 3a shows that 648
 649 the average monthly difference between the SBUV SCO 649
 650 derived from the version 6 archive and the measured SCO is 650
 651 14 DU, nearly twice as large as the difference calculated 651
 652 using SAGE. Every month shows SBUV SCO integrals 652
 653 higher than the observations. On the other hand, with the 653
 654 empirical correction, the agreement between the EC-SBUV 654
 655 SCO and the measured SCO is comparable to the agreement 655
 656 between the SAGE and measured SCO. 657

656 [34] Table 3b and Figure 10b summarize the measure- 656
 657 ments at Wallops Island. The amplitude of the seasonal 657
 658 cycle is less than that at Hohenpeissenberg and is captured 658
 659 by the all three data sets. As with Hohenpeissenberg, the 659
 660 four months of the greatest differences (>10 DU) between 660
 661 the SAGE and Dobson-ozonesonde SCO, (February, July, 661
 662 September, and November) all show higher SAGE amounts. 662
 663 Without the empirical correction, the SBUV integrals are 663
 664 significantly higher than both the measured and SAGE SCO 664
 665 values. With the correction, the EC-SBUV SCO is once 665

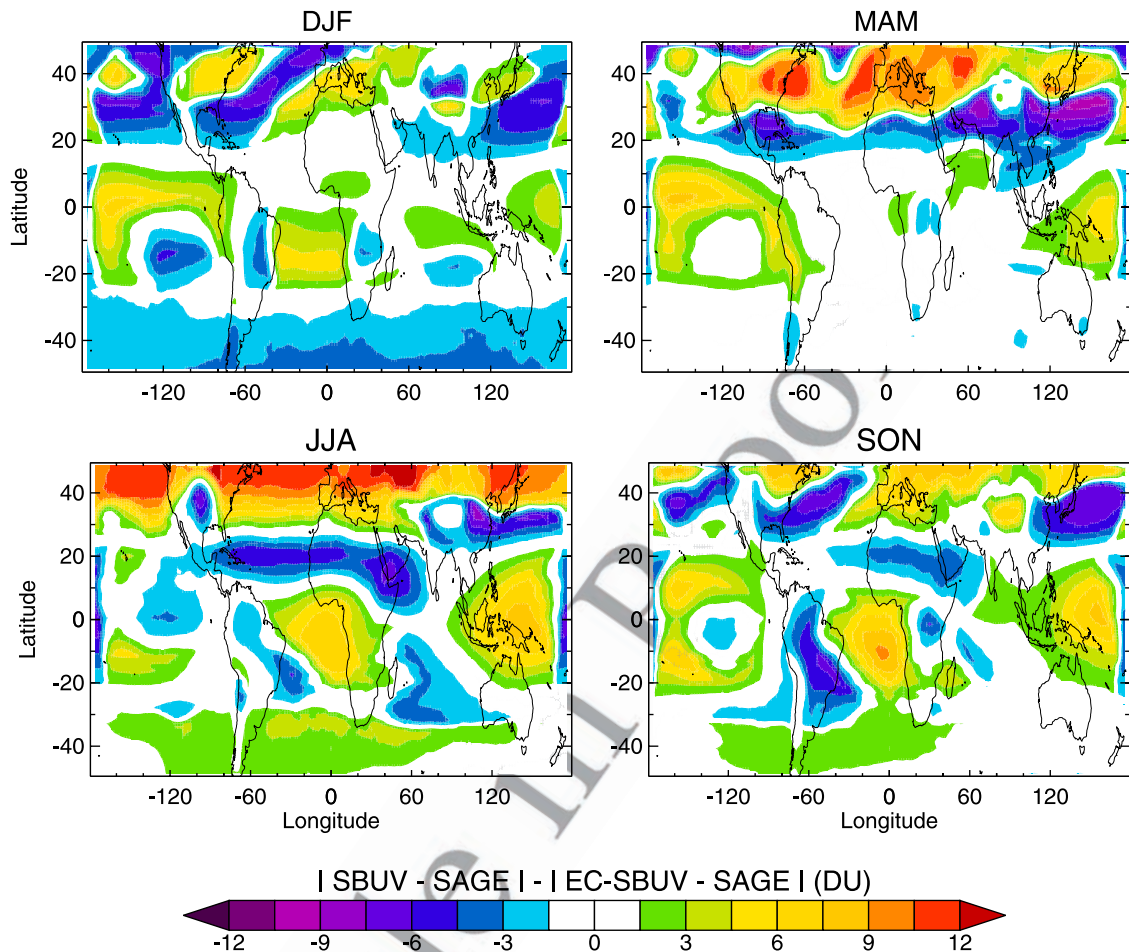


Figure 9. Distribution of $|SBUV-SAGE| - |EC-SBUV-SAGE|$. Regions with positive values show where the empirical correction has brought the SBUV fields closer to the stratospheric column ozone fields generated using SAGE measurements.

666 again slightly better than the agreement found between the
 667 observed SCO than the SAGE SCO values.

668 [35] Figure 11 shows monthly mean EC-SBUV SCO
 669 values compared with the ground-based/in situ SCO at
 670 the stations listed in Table 2. For each station, monthly
 671 EC-SBUV SCO values (open triangles) are plotted with

monthly ozonesonde/ground-based SCO values (asterisks). 672
 Table 4 summarizes the impact of the empirical correction on 673
 the data shown in Figure 11 by comparing the corresponding 674
 monthly mean error, standard deviation, and root-mean 675
 square error, for the EC-SBUV in these plots with both 676
 the ground-based/in situ measurements and with the SCO 677

t3.1 **Table 3a.** Seasonal Cycle of Observed SCO Over Hohenpeissenberg Compared With SCO Derived From Satellite Measurements^a

t3.2	Month	SCO ^b	SAGE	Diff	SBUV	Diff	EC-SBUV	Diff
t3.3	Jan	302	307	5	306	4	301	1
t3.4	Feb	321	311	10	329	8	323	2
t3.5	March	338	342	4	339	1	331	7
t3.6	April	338	338	0	350	12	340	2
t3.7	May	324	322	2	343	19	330	6
t3.8	June	307	294	13	327	20	314	7
t3.9	July	291	285	6	307	16	294	3
t3.10	Aug	278	276	2	292	14	282	4
t3.11	Sept	258	264	6	277	19	266	8
t3.12	Oct	254	256	2	267	13	258	4
t3.13	Nov	251	272	21	268	17	259	8
t3.14	Dec	268	290	22	288	20	282	14
t3.15	Average	294	296	8	308	14	298	6

t3.16 ^aAll values given in Dobson Units.

t3.17 ^bDobson-Ozonesonde.

t4.1 **Table 3b.** Seasonal Cycle of Observed SCO Over Wallops Island Compared With SCO Derived From Satellite Measurements^a

t4.2	Month	SCO ^b	SAGE	Diff	SBUV	Diff	EC-SBUV	Diff	t4.2
t4.3	Jan	285	280	5	290	5	285	0	t4.3
t4.4	Feb	286	304	18	301	15	293	7	t4.4
t4.5	March	304	303	1	314	10	306	1	t4.5
t4.6	April	308	310	2	320	12	308	0	t4.6
t4.7	May	293	299	6	313	20	300	7	t4.7
t4.8	June	285	281	4	294	9	282	3	t4.8
t4.9	July	264	274	10	279	15	271	7	t4.9
t4.10	Aug	258	259	1	272	14	267	9	t4.10
t4.11	Sept	246	257	11	263	17	257	11	t4.11
t4.12	Oct	250	257	7	259	9	253	3	t4.12
t4.13	Nov	244	258	14	256	12	249	5	t4.13
t4.14	Dec	268	262	6	272	4	266	2	t4.14
t4.15	Average	274	279	7	286	12	278	5	t4.15

t4.16 ^aAll values given in Dobson Units.

t4.17 ^bDobson-Ozonesonde.

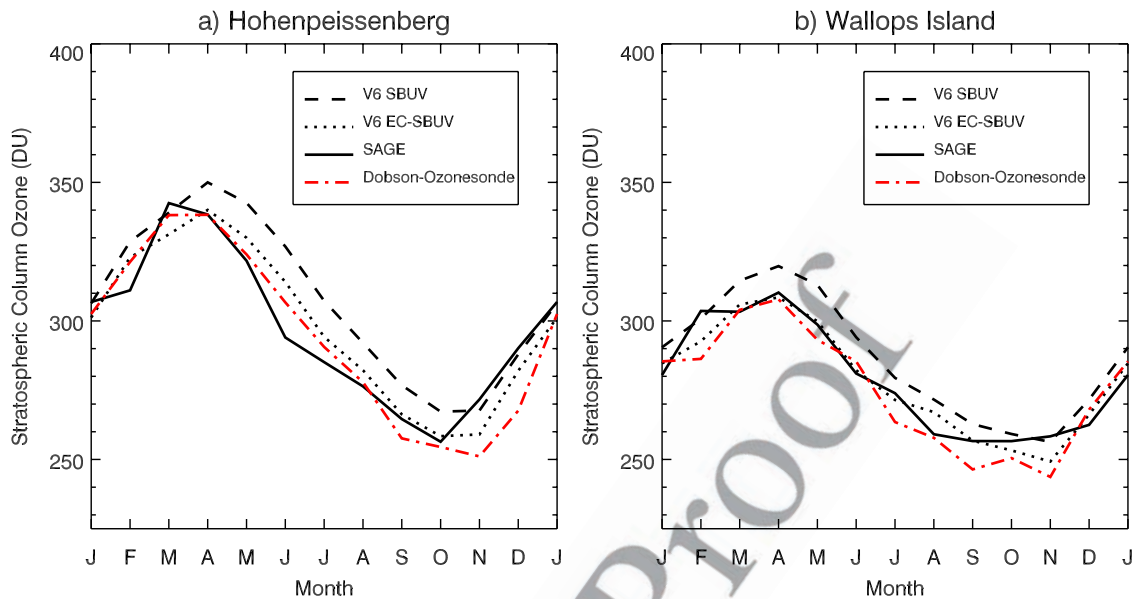


Figure 10. Seasonal cycle of SCO at Hohenpeissenberg, Germany, and Wallops Island, United States. The Dobson-ozonesonde values are plotted as thick dash-dotted (red) line; the satellite-derived (black) lines show SAGE SCO (thin solid line) and SBUV SCO (dashed line) and the EC-SBUV SCO (dotted line).

678 derived from the archived SBUV profiles (not plotted in
679 Figure 11). We see from this table that the empirical
680 correction has reduced the mean difference by an overall
681 average of 4 DU. Thus, in addition to improvements at
682 Hohenpeissenberg and Wallops Island described earlier,
683 there is also better agreement of the EC-SBUV SCO with
684 the ground-based/in situ SCO than the archived SBUV
685 SCO at almost every station where enough ozonesonde
686 data are available to perform such analyses.

688 6. Discussion

689 [36] It is generally agreed that stratospheric ozone distri-
690 butions derived from SAGE, MLS and HALOE provide
691 better vertical resolution than SBUV and that these datasets
692 have undergone extensive validation [WMO, 1999]. The
693 objective of this study is to show that the resultant SCO
694 fields derived using SBUV data that have been modified by
695 the empirical correction described by *Fishman et al.* [2003]
696 provide a SCO dataset that is comparable in accuracy to one
697 of these other instruments, SAGE. Validation of the TOR
698 derived from the use of TOMS can be done only by
699 comparing these derived data with measurements from only
700 a handful of available ozonesonde sites. Such studies have
701 already been performed. For example, we point to the
702 detailed study by *Sun* [2002] that summarizes all published
703 techniques prior to the EC-TOR data set described by
704 *Fishman et al.* [2003].

705 [37] As an alternative to a direct validation of the TOR
706 product that is derived from the empirical correction meth-
707 odology, this study has concentrated on the robust strato-
708 spheric ozone data set from SBUV to provide additional
709 insight into the accuracy of the resultant EC-TOR fields
710 derived using these SCO fields in conjunction with coinci-
711 dent TOMS total ozone measurements. The SCO fields
712 respond to large-scale forcing, and it is important that the

large-scale features picked up by different instruments are
713 consistent with validation measurements and with each
714 other. If these facts are verifiable, then we can assume that
715 the smaller scale variability, which is solely the result of the
716 greater spatial resolution of TOMS, is, in fact, a true
717 tropospheric feature.
718

[38] Unlike previous studies that look at TOR information
719 only at low latitudes, this EC-TOR technique provides
720 information at middle latitudes where there are considerably
721 more SAGE and ozonesonde profiles. We have shown that
722 the SCO derived from SBUV data after the empirical
723 correction has been applied improves the amount of ozone
724 in SBUV Layer 3 and also provides excellent agreement
725 with the SCO derived from the SAGE data set. The regions
726 of greatest difference between the SCO distributions derived
727 from the two different data sets coincides with regions
728 where the height of the tropopause is most difficult to
729 define [*Fishman et al.*, 1990; *Pierce et al.*, 2003].
730

731 7. Summary and Conclusions

[39] We have completed an in-depth analysis of the
732 distribution of stratospheric ozone using SBUV profile data
733 that have been modified according to the “empirical cor-
734 rection” described by *Fishman et al.* [2003]. We have found
735 the following: (1) The empirical correction improves the
736 calculated SCO relative to the archived SBUV (version 6)
737 profiles as compared to ozonesonde data; (2) at the limited
738 number of stations for which long-term ozonesonde records
739 exist, the SCO derived from the EC-SBUV data agree with
740 the ozonesonde data as well as SCO derived from SAGE
741 measurements; (3) over the 50°N–50°S domain for which a
742 climatology has been derived, the SCO seasonal distributions
743 using the EC-SBUV database are similar to those derived
744 from SAGE measurements; and (4) regions where the SAGE
745 and SBUV distributions differ the most are in locations where
746

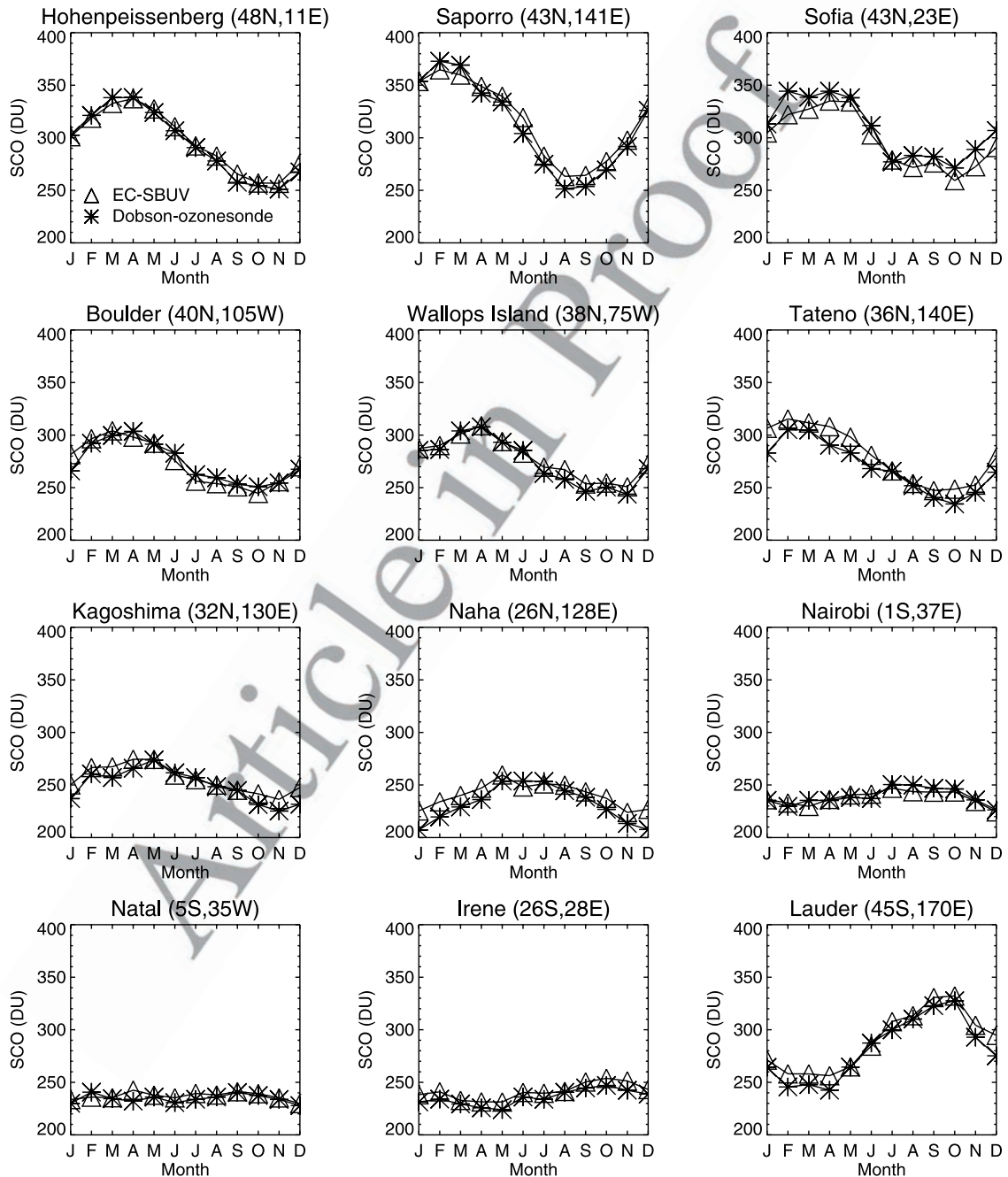


Figure 11. Monthly mean stratospheric column ozone derived from EC-SBUV and Dobson-ozonesonde measurements. The triangles are the EC-SBUV SCO and the asterisks are Dobson-ozonesonde SCO.

t5.1 **Table 4.** Monthly Mean Error, Standard Deviation, and RMSE for Stratospheric Column Ozone^a

t5.2	Station	Empirically Corrected SBUV			SBUV From V6 Archive		
		ME	SDE	RMSE	ME	SDE	RMSE
t5.4	Hohenpeissenberg, Germany	2.27	4.24	4.66	11.60	5.73	12.83
t5.5	Sapporo, Japan	4.73	7.47	8.57	10.64	9.56	14.03
t5.6	Sofia, Bulgaria	-10.35	6.31	11.98	-2.21	8.64	8.56
t5.7	Boulder, Colorado	-0.33	6.63	6.35	9.60	5.95	11.16
t5.8	Wallops Island, Virginia	3.33	3.82	4.94	11.20	2.59	11.47
t5.9	Tateno, Japan	10.91	6.22	12.61	18.38	7.74	19.82
t5.10	Kagoshima, Japan	6.17	7.45	8.58	12.75	6.68	14.27
t5.11	Naha, Japan	8.61	8.61	11.18	13.03	8.29	15.26
t5.12	Nairobi, Kenya	-1.12	3.46	3.50	1.24	1.71	2.05
t5.13	Natal, Brazil	2.52	3.55	4.23	6.21	4.45	7.54
t5.14	Irene, South Africa	5.60	2.10	5.95	7.78	2.49	8.14
t5.15	Lauder, New Zealand	7.96	6.15	9.90	7.83	5.00	9.18

t5.16 ^aAll values given in Dobson Units.

747 strong jet stream activity is taking place, suggesting that
748 neither can provide as accurate a data set as desired.

749 [40] The study by Sun [2002] has already provided a
750 comprehensive analysis of the utility and the limitations for
751 a number of studies that use a residual technique to infer
752 tropospheric ozone from TOMS total ozone measurements.
753 The EC-TOR data set described by Fishman et al. [2003]
754 was not included in that analysis, but, in general, the same
755 large-scale patterns seen by Fishman et al. [1990] and
756 subsequent residual methods again show up in TOR depic-
757 tions in the 2003 paper. The primary difference is the much
758 higher spatial resolution highlighted in EC-TOR data, which
759 is due to the much greater number TOMS measurements
760 used in the EC-TOR method.

761 Appendix A

762 [41] The primary rationale that prompted this study was
763 to find an alternative methodology to validate the tropo-
764 spheric ozone residual data set described by Fishman et al.
765 [2003]. As pointed out by Fishman et al. [2003], an
766 interactive comment presented in response to deLaat and
767 Aben [2003], there are no measurements available to vali-
768 date the regional nature of elevated TOR amounts high-
769 lighted in the Fishman et al. paper. On the other hand,
770 robust data sets do exist that can be used to validate the
771 other quantity that must be generated to calculate the TOR,
772 namely the SCO.

773 [42] During the course of our research, however, NOAA
774 and NASA scientists were incorporating improvements into
775 SBUV retrievals and eventually released version 8 of the
776 data SBUV archive. The primary improvement in the
777 version 8 algorithm is the incorporation of the Logan
778 [1999] climatology as a priori information in the lowest
779 three layer, exactly as described in our empirical correction.
780 Although the analysis of the SCO distribution would
781 provide the most up-to-date comparison of how these fields
782 compare with currently available ozonesonde and SAGE
783 measurements, the SCO distributions derived with these
784 more recently archived SBUV data would not be consistent
785 with the data that went into the generation of the TOR fields
786 discussed by Fishman et al. [2003].

787 [43] Furthermore, since the release of version 8 SBUV,
788 only a handful of unpublished papers have been presented

describing the accuracy of the data set [McPeters et al., 789
2003; Deland et al., 2004]. On the other hand, version 6 790
SBUV is a data set that has been used in numerous other 791
studies and has been compared previously with other 792
satellite measurements, as well as with ozonesonde meas- 793
urements [e.g., MCPeters et al., 1994]. The additional 794
analysis provided in the current study provides further 795
insight into the shortcomings of the version 6 data set and 796
proposes a method to remedy the observed problems, which 797
were essentially implemented during the course of the 798
current research and resulted in the release of version 8. 799

[44] We compared version 6 and version 8 SBUV ozone 800
columns above 63 hPa derived from NIMBUS-7 (1979- 801
1990) and NOAA-11 (1989–2000) measurements. For the 802
NOAA-11 SBUV/2 data, (version 8–version 6) mean differ- 803
ences averaged over 10° latitude bands between 50°S and 804
50°N are approximately 1% (~2DU). The 1-sigma standard 805
deviation is approximately 2.5%. For the NIMBUS-7 SBUV 806
data, which were used for less than one fourth of the SCO 807
calculations in this study (1985–1989), mean differences 808
averaged over 10° latitude bands between 50°S and 50°N 809
are approximately 3% (~6 DU). The 1-sigma standard 810
deviation is approximately 3%. The correlation between 811
version 6 and version 8 column ozone above 63 hPa 812
is greater than 0.90 for each year of data. In our compar- 813
ison of SBUV SCO with SAGE, The EC-SBUV profiles 814
should be an excellent approximation of the version 815
8 SBUV profiles, particularly for the NOAA-11 instrument 816
data. 817

[45] Finally, a companion paper, Fishman et al. [2005], 818
discusses the interannual variability (IAV) of the SCO fields 819
discussed in this paper and the regional nature of IAV found 820
in the corresponding TOR data set. The Fishman et al. 821
[2005] study provides additional credibility to the SCO 822
derived in the present study by showing that these data 823
are consistent with previous stratospheric ozone IAV studies 824
that have used TOMS total ozone and SAGE ozone profile 825
measurements to provide insight into the relationship be- 826
tween the quasi-biennial oscillation and the dynamics that 827
impact the distribution of stratospheric ozone. 828

[46] **Acknowledgments.** SBUV/2 data were obtained from NOAA/ 829
NESDIS with support from the NOAA Climate and Global Change 830
Program Atmospheric Chemistry Element. We thank T. Zenker for his 831
work on the vertical interpolation of the SBUV data and V. Brackett for 832
maintaining the ozonesonde database. We also thank the anonymous 833
referees whose comments greatly improved the manuscript. Map colors 834
were taken from www.ColorBrewer.org by Cynthia A. Brewer, Geography, 835
Pennsylvania State University. 836

References 837

- Beekman, M., et al. (1997), Regional and global tropopause fold occurrence 838
and related ozone flux across the tropopause, *J. Atmos. Chem.*, 28, 29–44. 839
Bhartia, P. K., R. D. McPeters, C. L. Mateer, L. E. Flynn, and 840
C. Wellemeyer (1996), Algorithm for the estimation of vertical ozone 841
profiles from the backscatter ultraviolet technique, *J. Geophys. Res.*, 842
101, 18,793–18,806. 843
Bremer, H., et al. (2004), Spatial and temporal variation of MOPPITT CO 844
in Africa and South America: A comparison with SHADOZ ozone and 845
MODIS aerosol, *J. Geophys. Res.*, 109, D12304, doi:10.1029/ 846
2003JD004234. 847
Chatfield, R. B., and H. Harrison (1977), Tropospheric ozone: 2. Variations 848
along a meridional band, *J. Geophys. Res.*, 82, 5969–5976. 849
Crutzen, P. J. (1974), Photochemical reactions initiated by and influencing 850
ozone in unpolluted tropospheric air, *Tellus*, 26, 47–57. 851
deLaat, A. T. J., and I. Aben (2003), Problems regarding the tropospheric 852
O₃ residual method and its interpretation in Fishman et al. (2003), *Atmos.* 853
Chem. Phys. Discuss., 3, 5777–5802. 854

- 855 Deland, M. T., et al. (2004), Long-term SBUV and SBUV/2 instrument
856 calibration for version 8 ozone data, in *Proceedings of the XX Quadren-*
857 *ennial Ozone Symposium, 1–8 June 2004, Kos, Greece*, edited by C. S.
858 Zerefos, pp. 321–322, Univ. of Athens, Athens, Greece.
- 859 Diab, R. D., A. M. Thompson, K. Mari, L. Ramsay, and G. J. R. Coetzee
860 (2004), Tropospheric ozone climatology over Irene, South Africa, from
861 1990 to 1994 and 1998 to 2002, *J. Geophys. Res.*, *109*, D20301,
862 doi:10.1029/2004JD004793.
- 863 Fabian, P., and P. G. Pruchniewicz (1973), Meridional distribution of tropo-
864 spheric ozone from ground-based registrations between Norway and
865 South Africa, *Pure Appl. Geophys.*, *106*(5–7), 1027–1035.
- 866 Fabian, P., and P. G. Pruchniewicz (1977), Meridional distribution of ozone
867 in the troposphere and its seasonal variations, *J. Geophys. Res.*, *82*,
868 2063–2073.
- 869 Fioletov, V. E., J. B. Kerr, E. W. Hare, G. J. Labow, and R. D. McPeters
870 (1999), An assessment of the world ground-based total ozone network
871 performance from the comparison with satellite data, *J. Geophys. Res.*,
872 *104*, 1737–1747.
- 873 Fishman, J., and A. E. Balok (1999), Calculation of daily tropospheric
874 ozone residuals using TOMS and empirically improved SBUV measure-
875 ments: Application to an ozone pollution episode over the eastern United
876 States, *J. Geophys. Res.*, *104*, 30,319–30,340.
- 877 Fishman, J., and P. J. Crutzen (1978), The origin of ozone in the tropo-
878 sphere, *Nature*, *274*, 855–858.
- 879 Fishman, J., S. Solomon, and P. J. Crutzen (1979), Observational and
880 theoretical evidence in support of a significant in-situ photochemical
881 source of tropospheric ozone, *Tellus*, *31*, 432–446.
- 882 Fishman, J., C. E. Watson, J. C. Larsen, and J. A. Logan (1990), Distribu-
883 tion of tropospheric ozone determined from satellite data, *J. Geophys.*
884 *Res.*, *95*, 3599–3617.
- 885 Fishman, J., V. G. Brackett, E. V. Browell, and W. B. Grant (1996a),
886 Tropospheric ozone derived from TOMS/SBUV measurements during
887 TRACE-A, *J. Geophys. Res.*, *101*, 24,069–24,082.
- 888 Fishman, J., J. M. Hoell Jr., R. D. Bendura, R. J. McNeal, and V. W. J. H.
889 Kirchoff (1996b), NASA GTE TRACE-A experiment (September–
890 October 1992): Overview, *J. Geophys. Res.*, *101*, 23,865–23,879.
- 891 Fishman, J., A. E. Wozniak, and J. K. Creilson (2003), Global distribution
892 of tropospheric ozone from satellite measurements using the empirically
893 corrected tropospheric ozone residual technique: Identification of the
894 regional aspects of air pollution, *Atmos. Chem. Phys.*, *3*, 893–907.
- 895 Fishman, J., J. K. Creilson, A. E. Wozniak, and P. J. Crutzen (2005),
896 Interannual variability of stratospheric and tropospheric ozone deter-
897 mined from satellite measurements, *J. Geophys. Res.*, in press.
- 898 Hudson, R. D., and A. M. Thompson (1998), Tropical tropospheric ozone
899 from Total Ozone Mapping Spectrometer by a modified residual method,
900 *J. Geophys. Res.*, *103*, 22,129–22,145.
- 901 Kaye, J. A., and J. Fishman (2003), Stratospheric ozone observations, in
902 *Handbook of Climate, Weather, and Water: Chemistry, Impacts, and*
903 *Applications*, edited by T. D. Potter and B. Colman, pp. 385–404, John
904 Wiley, Hoboken, N. J.
- 905 Logan, J. A. (1985), Tropospheric ozone: Seasonal behavior, trends and
906 anthropogenic influence, *J. Geophys. Res.*, *90*, 10,463–10,482.
- 907 Logan, J. A. (1999), An analysis of ozonesonde data for the troposphere:
908 Recommendations for testing 3-D models, and development of a gridded
909 climatology for tropospheric ozone, *J. Geophys. Res.*, *104*, 16,115–
910 16,149.
- 911 McPeters, R. D., D. F. Heath, and P. K. Bhartia (1986), Average ozone
912 profiles for 1979 from the NIMBUS 7 SBUV instrument, *Geophys. Res.*
913 *Let.*, *13*, 1213–1216.
- McPeters, R. D., T. Miles, L. E. Flynn, C. G. Wellemeyer, and J. M. 914
Zawodny (1994), Comparison of SBUV and SAGE II ozone profiles:
915 Implications for ozone trends, *J. Geophys. Res.*, *99*, 20,513–20,524. 916
- McPeters, R. D., et al. (2003), Ozone climatological profiles for version 8 917
TOMS and SBUV retrievals, *Eos Trans. AGU*, *84*(46), Fall Meet. Suppl., 918
Abstract A21D-0998. 919
- Newchurch, M. J., X. Liu, and J. H. Kim (2001), Lower-tropospheric ozone 920
(LTO) derived from TOMS near mountainous regions, *J. Geophys. Res.*, 921
106, 20,403–20,412. 922
- Newchurch, M. J., D. Sun, J. H. Kim, and X. Liu (2003), Tropical tropo- 923
spheric ozone derived using clear-cloudy pairs (CCP) of TOMS measure- 924
ments, *Atmos. Chem. Phys.*, *3*, 683–695. 925
- Pierce, R. B., et al. (2003), The Regional Air Quality Modeling System 926
(RAQMS) predictions of the tropospheric ozone budget over east Asia, 927
J. Geophys. Res., *108*(D21), 8825, doi:10.1029/2002JD003176. 928
- Prinn, R. G. (1988), Toward an improved network for determination of 929
tropospheric ozone climatology and trend, *J. Atmos. Chem.*, *6*, 281–298. 930
- SPARC (1998), Assessment of trends in the vertical distribution of ozone, 931
Rep. 43, World Meteorol. Org. Global Ozone Res. and Monit. Project, 932
Geneva. 933
- Sun, D. (2002), Tropical tropospheric ozone: New methods, comparisons, 934
and model evaluation of controlling processes, dissertation, 174 pp., Dep. 935
of Atmos. Sci., Univ. of Ala., Huntsville. 936
- Thompson, A. M., et al. (2003), Southern Hemisphere Additional Ozone- 937
sondes (SHADOZ) 1998–2000 tropical ozone climatology: 2. Tropo- 938
spheric variability and the zonal wave-one, *J. Geophys. Res.*, *108*(D2), 939
8241, doi:10.1029/2002JD002241. 940
- Vukovich, F. M., V. Brackett, J. Fishman, and J. E. Sickles II (1996), On the 941
feasibility of using the tropospheric ozone residual for nonclimatological 942
studies on a quasi-global scale, *J. Geophys. Res.*, *101*, 9093–9105. 943
- Vukovich, F. M., V. Brackett, J. Fishman, and J. E. Sickles II (1997), A 944
5-year evaluation of the tropospheric ozone residual at nonclimatologi- 945
cal periods, *J. Geophys. Res.*, *102*, 15,927–15,932. 946
- Wang, H. J., D. M. Cunnold, L. W. Thomason, J. M. Zawodny, and G. E. 947
Bodeker (2002), Assessment of SAGE version 6.1 ozone data quality, 948
J. Geophys. Res., *107*(D23), 4691, doi:10.1029/2002JD002418. 949
- Wang, Y. H., J. A. Logan, and D. J. Jacobs (1998), Global simulation of 950
O-3-NOx-hydrocarbon chemistry: 3. Origin of tropospheric ozone and 951
effects of non-methane hydrocarbon, *J. Geophys. Res.*, *103*, 10,757– 952
10,767. 953
- World Meteorological Organization (1999), Scientific assessment of ozone 954
depletion: 1998, *Rep. 44*, 732 pp., Global Ozone Res. and Monit. Project, 955
Geneva. 956
- World Meteorological Organization (2003), Scientific assessment of ozone 957
depletion: 2002, *Rep. 47*, 498 pp., Global Ozone Res. and Monit. Project, 958
Geneva. 959
- Ziemke, J. R., S. Chandra, and P. K. Bhartia (1998), Two new methods 960
for deriving tropospheric column ozone from TOMS measurements: 961
Assimilated UARS MLS/Haloe and convective-cloud differential techni- 962
ques, *J. Geophys. Res.*, *103*, 22,115–22,127. 963
-
- J. K. Creilson and J. Fishman, NASA Langley Research Center, Mail 964
Stop 401A, Hampton, VA 23681, USA. (j.k.creilson@larc.nasa.gov; jack. 966
fishman@nasa.gov) 967
- P.-H. Wang, NASA Langley Research Center, Mail Stop 910, Hampton, 968
VA 23681, USA. (p.wang@larc.nasa.gov) 969
- A. E. Wozniak, NASA Goddard Space Flight Center, Code 613.3, 970
Greenbelt, MD 20771, USA. (a.e.wozniak@larc.nasa.gov) 971